On the micro- and mesomodeling of the interfaces between laminate plies

P.Ladevèze*, D.Marsal*, G.Lubineau*

*LMT-Cachan, E.N.S. Cachan / Université Paris 6 / C.N.R.S.
61 Avenue du Président Wilson, 94235 Cachan, France
email: ladeveze@lmt.ens-cachan.fr, marsal@lmt.ens-cachan.fr, lubineau@lmt.ens-cachan.fr

ABSTRACT

A bridge between the micro- and mesomechanics of laminates is being developed. The objective is to improve the calculation of the final fracture of laminated structures. Previous works have shown that under plane loading the mesomodel can be interpreted as an homogenized model, thus leading to the derivation of rather complete micro-meso relations. The present paper goes further by considering out-of-plane loading. Here, we focus only on the interface model which connects two adjacent plies. In particular, the micro-meso relations obtained quantify the impact of the microcracking of adjacent plies on the delamination of their interface.
KEYWORDS: LAMINATES, DAMAGE, INTERFACE, DELAMINATION, MICRO-MESO

1. INTRODUCTION

In order to benefit from the damage tolerance of laminates, industrial structures require models and simulations capable of predicting the intensities of the damage processes and their evolutions up to final failure under complex loading conditions. Moreover, these models should enable the use of simulations in replacement of the numerous tests formerly used in the design of high-gradient zones.

The upcoming solutions are rooted in more than 20 years of intense developments which can be split into two main families. On the one hand, the micromechanics models are based on the fiber's scale. Directly linked to the observations of the degradation micromechanisms, these models have led to numerous theoretical and experimental works, focusing mainly on the study of the phenomenon of matrix microcracking (Flaggs and Kural, 82 [1]; Hashin, 85 [2]; Boniface et al., 87 [3]; Laws and Dvorak, 88 [4], Nairn and Hu, 94 [5]; Joff and Varna, 99 [6]). A second major phenomenon, local delamination, has also been investigated (Crossman and Wang, 82 [7]; Nairn and Hu, 92 [8], Berthelot and Corre, 00 [9]). A review of micromechanics models can be found in (Nairn, 00 [10]). These approaches, which focus on the microscale, provide a good understanding of the damage mechanisms, but they do not provide solutions for structural simulation and macro failure prediction.

On the other hand, continuum damage mechanics models have enabled the construction of larger-scale models (Talreja, 80 [11]; Renard and Jeggy, 89 [12]). The main purpose of these models, which are also linked to experimental observations (but on the specimen's scale), is structural simulation and macro failure prediction. Within this category, our own approach relies on a Damage Mesomodel for Laminates (DML) (Ladevèze, 86 [13]; Ladevèze, 89 [14]; Herakovich, 98 [15]) based on the scale of the ply – also called the mesoscale – as an intermediary between the microscale of the fiber and the macroscale of the laminate. The effects of the various micromechanisms are included in the damage mesovariables, but their relation to micromechanics is only qualitative.

Our goal is to improve the accuracy and robustness of the damage modeling of laminates in order to achieve satisfactory prediction of the initiation of microcracks and of their propagation until final fracture. We are especially concerned with engineering structures containing high-gradient zones, hence our efforts, as part of our current works, to bridge the micro- and mesomechanics of laminates.

Initially, the single-layer model was studied under in-plane macroloading and in the cases of matrix microcracking (Ladevèze and Lubineau, 01 [16]; Ladevèze and Lubineau, 02 [17]) and local interlaminar delamination (Ladevèze and Lubineau, 02 [18]). It was proven that the damage mesoquantities (damage variables and associated damage forces) can be viewed as homogenized microquantities which are independent of the stacking sequence. This led to the

derivation of micro-meso relations for the damage variables and the forces. This paper follows the same approach, but goes one step further by considering out-of-plane loading situations, in which the interface model which connects two adjacent plies is of primary importance.

In Section 2, we first describe the microphenomenology adopted and the standard mesomodel. Then, we give a general overview of the method, from the general principle to the fundamental micro-meso relations and their practical use. In Section 3, we focus on the basic problem of the interface and delimit the domain of study. Several important properties derived from a virtual testing procedure enable us to quantify the interaction between the microcracking and local delamination mechanisms. This allows us to conclude that the damage microvariables and mesovariables are directly connected, which leads the way to various descriptions of damage and its evolution. These results are currently being used as guidelines for the implementation of an improved mesomodel.

2. THE BRIDGE BETWEEN THE MICRO- AND MESOMECHANICS OF LAMINATES

2.1 Microphenomenology

At present, micro-meso relations are restricted to the four micromechanisms of degradation illustrated in Fig. 1.

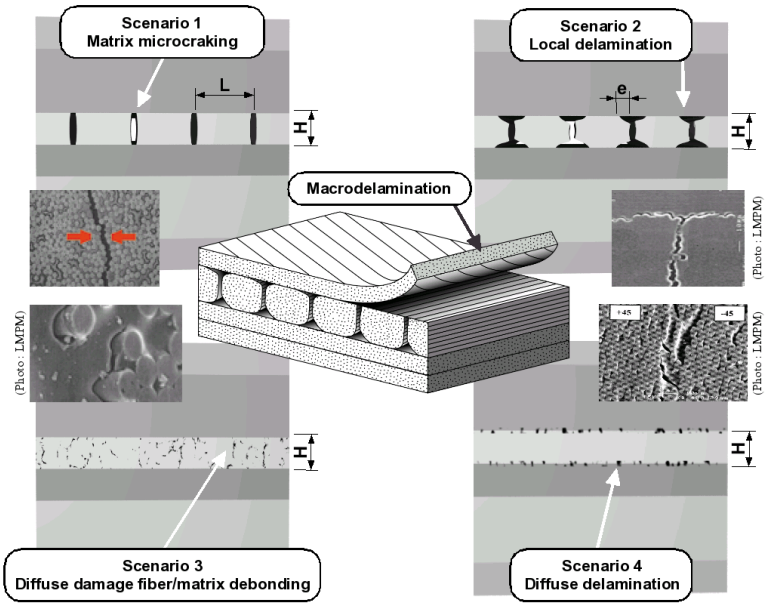

Fig. 1. Mechanisms of degradation on the microscale

- **Scenario 1**: transverse microcracking. These cracks are assumed to span the whole thickness of the ply and to follow a periodic pattern, at least locally. This scenario is quantified by the cracking rate ρ such that:

$$\rho = \frac{H}{L}$$

- **Scenario 2**: local delamination. These cracks, which are initiated at the tips of the transverse microcracks, are assumed to follow a periodic pattern. This scenario is quantified at each transverse crack's tip by a local delamination rate τ such that:

$$\tau = \frac{e}{H}$$

- **Scenario 3**: diffuse damage. Degradation mechanisms such as fiber/matrix debonding

introduce a quasi-homogenous loss of stiffness in the ply.

- **Scenario 4**: diffuse delamination. Degradation mechanisms such as the occurrence of microvoids and microdecohesions, whose scale is smaller than that of local delamination, introduce a quasi-homogenous loss of stiffness in the interface.

The first two mechanisms are common and have been thoroughly investigated by the micromechanics community in the case of laminated composites. The last two mechanisms have long been included in the DML, but not in micromechanics. These mechanisms are essential to explain certain kinds of behavior, such as the significant loss of stiffness of shear-loaded laminates (Lagattu and Lafarie-Frenot, 00 [19]). The evolution of the microvariables ρ and τ is governed by energy release rates in the framework of fracture mechanics or finite fracture mechanics.

In most practical cases, the sequence of scenarios is as follows: Damage is initiated by Scenarios 3 and 4. Then, the accumulation of fiber-matrix debonding instances followed by their coalescence leads to transverse microcracking (Scenario 1). The competition between transverse microcracking and local delamination ends up with the saturation of Scenario 1 and is relayed by the catastrophic development of Scenario 2. Finally, this last scenario, just like Scenario 4, can lead to macroscopic interlaminar debonding due to coalescence under out-of-plane macroloading.

2.2 Standard damage mesomodel for long-fiber laminates

The standard DML is based on two hypotheses (Ladevèze, 89 [13]). The first assumption is that the behavior of any stacking sequence subjected to any loading can be predicted on the mesoscale through two mesoconstituents which are continuous media: the single layer and the interface (Fig. 2).

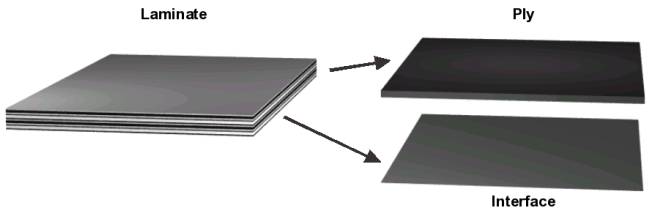

Fig. 2. Decomposition of a laminated composite into mesoconstituents

The damage state of each mesoconstituent is quantified by damage variables linked to the mesoconstituent's loss of stiffness. Traditionally, the evolution of these mesovariables depends on damage forces which quantify the evolution of the mesoconstituent's energy as a function of damage. The damage evolution laws of the ply and of the interface must be valid regardless of the stacking sequence and loading conditions.

The interface is a surface entity representing the thin layer of matrix which exists between two adjacent plies and is characterized by their relative orientation. It provides for the transfer of stresses and displacements from one ply to the next. Its stiffness is the ratio of the shear modulus of the matrix to its thickness, which is assumed to be one-fifth of the thickness of an elementary ply.

The second assumption is that the damage variables are constant throughout the thickness of each single layer, but can vary from one layer to the next. Preliminary identifications were carried out in previous works for the single layer (Ladevèze and Le Dantec, 92 [20]; Allix and Ladevèze, 92 [21]); Allix et al., 96 [22]) and for the interface (Allix et al., 98 [23]). A review of the most recent works dealing with delamination can be found in (Allix, 02 [24]).

2.3 The equivalence principle

The key to our approach is to link the mesomodel to the micromechanical models from an energy point of view. Indeed, one of the objectives of deriving micro-meso relations is to study the evolution of damage, and the main fracture criteria themselves are based on energy concepts. Consequently, in our multiscale approach, the potential energy stored in any part of a complete structure must be the same on the microscale and on the mesoscale, as illustrated in Fig. 3.

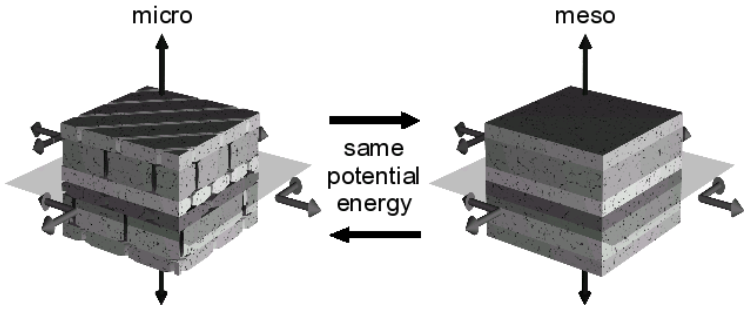

Fig. 3. Energy equivalence between the micro and meso interpretations of damage

The determination of the potential energy of the domain on the microscale involves the calculation of the stress field at any point of the domain. Since the thickness of a ply is about 150µm, one can imagine the huge size of the associated finite element problem for the complete structure. Moreover, one must be able to carry out the equivalence under any loading and for any stacking sequence, which makes this general problem inaccessible. Therefore, specific appropriate methods and hypotheses are required.

2.4 The method to build the micro-meso bridge

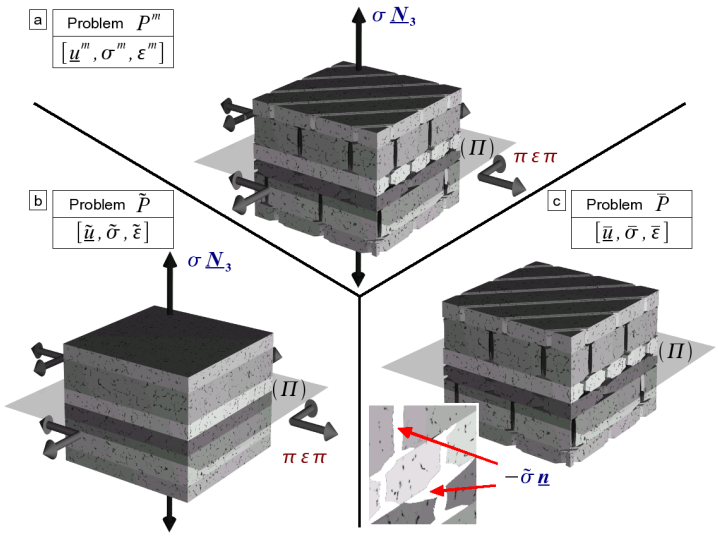

Fig. 4. Decomposition of the solution into a continuous solution and a discrete solution

First, under the assumption of linear elasticity, the exact solution $S_m[u_m,\sigma_m]$ is decomposed using a crack closure method (Fig. 4). A first trivial solution for the domain is obtained in the absence of discrete damage. This continuous solution $\hat{S}[\hat{u},\hat{\sigma}]$ verifies the boundary conditions of the domain. Then, a residual solution $\bar{S}[\bar{u},\bar{\sigma}]$ is obtained by subjecting the discretely damaged domain to a residual load $-\tilde{\sigma}.\underline{n}$ in the cracked area, $\underline{n}$ being the vector normal to the cracked area. Consequently, the combination of the two solutions, which is kinematically and statically admissible, is the exact solution. At this stage, the residual problem presents the same difficulties as the general problem.

Three more hypotheses are required: First, the residual load $-\tilde{\sigma}.\underline{n}$ is assumed to be ply-constant in the vicinity of a transverse crack. Second, Scenarios 3 and 4 are assumed to be locally homogeneous within each ply and each interface, and Scenarios 1 and 2 are assumed to be locally periodic. Third, the general problem is considered to be solved if two basic situations of equivalence are met, one for the ply and one for the interface, as shown in Fig. 5.

Remark 1: Under out-of-plane loading, the interactions between two adjacent plies must be taken into account. A third elementary problem, whose results are not presented here, can be introduced to deal with these phenomena (Ladevèze, Lubineau and Marsal, 03 [25]).

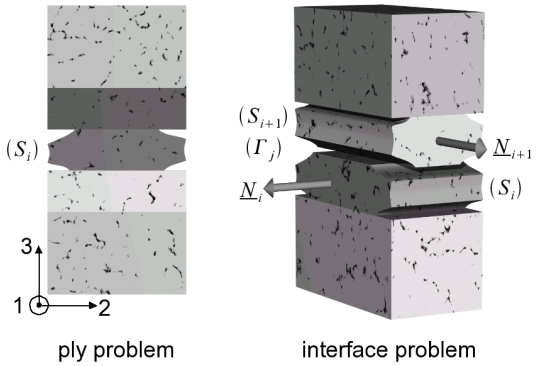

Fig. 5. Basic ply and interface problems

2.5 The fundamental micro-meso relation

For these basic problems, there is a strong link between the microsolution and the mesosolution. The plane part of the mesostrain and the out-of-plane part of the mesostress are the mean values of the corresponding microfields.

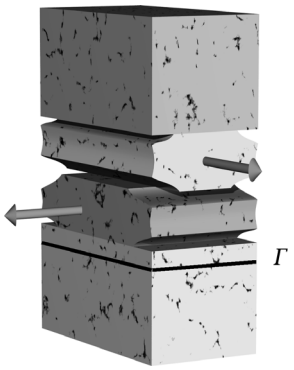

$$\pi\,\varepsilon_{meso}\,\pi\big|_{\Gamma} = \langle \pi\,\varepsilon_{micro}\,\pi \rangle_{\Gamma}$$
$$\sigma_{meso}\,\underline{N}_3\big|_{\Gamma} = \langle \sigma_{micro}\,\underline{N}_3 \rangle_{\Gamma}$$

As a result, it has been proven that the energy of an elementary mesoconstituent can be written as a quadratic form of the macroloading $\tilde{C}$ expressed in terms of the plane part of the strain and the out-of-plane part of the stress.

$$2E_p^{meso} = \tilde{C}^T A^{meso} \tilde{C} \qquad \tilde{C} = \left[\left[\tilde{\varepsilon}_{11}\ \tilde{\varepsilon}_{22}\ \tilde{\varepsilon}_{12}\right]\left[\tilde{\sigma}_{13}\ \tilde{\sigma}_{23}\ \tilde{\sigma}_{33}\right]\right]^T$$

$$2E_p^{micro} = \tilde{C}^T A^{micro} \tilde{C}$$

While the meso-operator A_{meso} is a function of the internal variables associated with the loss of stiffness of the mesoconstituents, the micro-operator A_{micro} is a function of the microdegradation variables based on the microphenomenology adopted in Section 1. These two operators should be the same for any stacking sequence, under any loading condition and for any level of microdamage. In practice, one reduces the damage domain by setting ρ in [0.0; 0.7] and τ in [0.0; 0.4]. Experiments show that for higher levels of microdegradation the material can be considered to be fully damaged.

In the following section, we will detail the virtual testing procedure which enables us to identify the interface's homogenized meso-operator from the microscale.

3. THE BASIC INTERFACE PROBLEM

3.1 Potential energy of the interface

In order to homogenize the microdegradations associated with an interface Γ_j between two damaged plies S_i and S_{i+1} whose fiber directions are $\underline{N}_i$ and $\underline{N}_{i+1}$ respectively, let us consider the 3D cell of Fig. 6. The angle between $\underline{N}_i$ and $\underline{N}_{i+1}$ is denoted θ. One can introduce a local reference frame of orthotropic directions $(\underline{N}_1,\underline{N}_2,\underline{N}_3)$ for the healthy interface; $\underline{N}_3$ is normal to the interface while $\underline{N}_1$ and $\underline{N}_2$ are the bisector directions associated with the angle θ. The external plies S"- and S"+ representing the remaining structure are homogenized and possibly damaged according to Scenario 3. With the exception of transverse cracks, each pair of vertical faces of the 3D cell must satisfy periodic conditions corresponding to Scenarios 1 and 2.

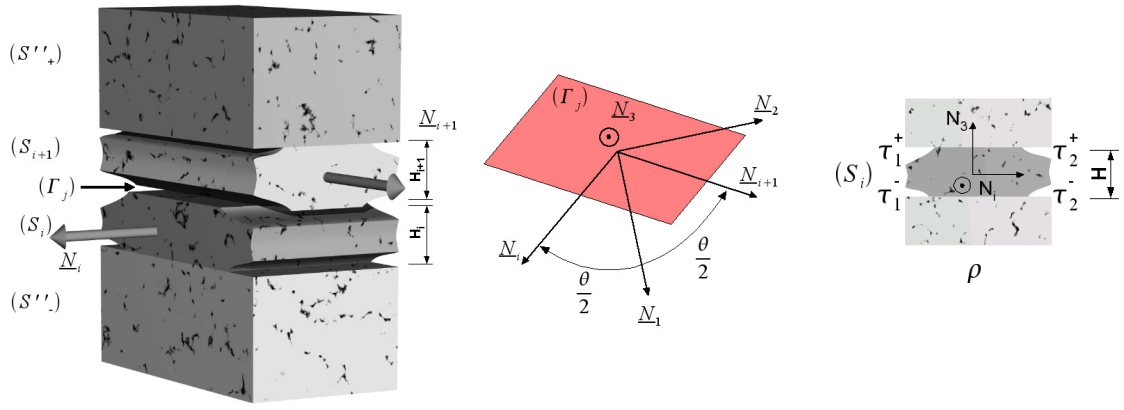

Fig. 6. The basic interface problem P^{int} and corresponding notations

The geometric parameters of the interface are the angle θ and the dimensionless quantities $(H_i/H_j, H_{i+1}/H_j)$ which quantify the unit thickness of the interface. The description of the state of microdegradation of the cell requires the microcracking rate and the four local delamination rates of each of the adjacent plies S_i and S_{i+1}:

$$\left((\rho, \tau_1^-, \tau_2^-, \tau_1^+, \tau_2^+)\Big|_{S_i} \;,\; (\rho, \tau_1^-, \tau_2^-, \tau_1^+, \tau_2^+)\Big|_{S_{i+1}} \right)$$

The delamination state can also be expressed using the ratio λ of the delaminated area of the interface to the total area of interface. The interface, being a surface entity with normal $\underline{N}_3$, is active only under out-of-plane loading conditions. Thus, the residual problem consists in loading the cracked area, whose normal vector is denoted $\underline{n}$, with the stresses $-\tilde{\sigma}.\underline{n}$ expressed in terms of out-of-plane stresses:

$$\tilde{C} = \left[\tilde{\sigma}_{13} \; \tilde{\sigma}_{23} \; \tilde{\sigma}_{33} \right]^T$$

According to the assumption of linear elasticity, the residual stresses can be decomposed into three elementary solicitations in the orthotropic basis of the interface. Consequently, one can express the residual solution as the sum of the three elementary solutions:

$$\bar{\sigma} = \bar{\sigma}^{13} + \bar{\sigma}^{23} + \bar{\sigma}^{33}$$

Result 1: the interface can be homogenized and its potential energy can be written as:

$$\frac{E^{micro}_{p\,interface}(j, \tilde{\sigma}\,\underline{N}_3)}{|\Gamma_j|} = -\frac{1}{2}\left[\tilde{\sigma}_{33}^2 \frac{(1+I_3)}{k_3} + \tilde{\sigma}_{13}^2 \frac{(1+I_1)}{k_1} + \tilde{\sigma}_{23}^2 \frac{(1+I_2)}{k_2} \right] + \; coupling\,terms$$

k_1, k_2 and k_3 are the initial elastic stiffness coefficients of the interface, possibly including initial diffuse damage. The three damage indicators I_1, I_2 and I_3 are functions of the microdegradation variables and are defined as the integrals of the strain energy over the

interface for each elementary problem:

$$I_i = \frac{k_i}{\left|\Gamma_j\right| \tilde{\sigma}_{i3}^2} \int_\Gamma Tr\left[\bar{\sigma}^{i3}\bar{\varepsilon}^{i3}\right] d\Gamma$$

3.2 Relations between the micro- and mesomodel

On the mesoscale, the energy of the interface has the following expression:

$$\frac{E^{meso}_{p\,interface}(j, \tilde{\sigma}\,\underline{N}_3)}{\left|\Gamma_j\right|} = \frac{-1}{2}\left[\frac{\tilde{\sigma}_{33}^2}{(1-D_3)k_3} + \frac{\tilde{\sigma}_{13}^2}{(1-D_1)k_1} + \frac{\tilde{\sigma}_{23}^2}{(1-D_2)k_2}\right]$$

D_1, D_2 and D_3 are the mesodamage variables associated with the loss of stiffness of the interface. This leads to the definition of two operators:

$$A^{meso}_{interface} : (D_3, D_2, D_1)$$

$$A^{micro}_{interface}\left((\rho, \tau_1^-, \tau_2^-, \tau_1^+, \tau_2^+)\big|_{S_i} \ , \ (\rho, \tau_1^-, \tau_2^-, \tau_1^+, \tau_2^+)\big|_{S_{i+1}}\right)$$

Prior to carrying out any identification between the micro- and meso-operators, one must verify the consistency of the homogenized operator with the hypotheses of the mesomodel.

Result 2: The homogenized operator is intrinsic to the interface.

One must evaluate the intrinsic properties of the homogenized operator with respect to the interface: for a given set of interface parameters (θ,H_i/H_j,H_{i+1}/H_j) the identified damage indicators should not depend on the stacking sequence. For convenience, the results are presented in terms of the loss of stiffness variables D_1, D_2 and D_3, which are related to the damage indicators by:

$$D_i = \frac{I_i}{1 + I_i}$$

In order to prove this property, let us consider the interface defined in Table 1. The orientations of the fibers refer to the direction $\underline{N}_1$ of the interface. H_{elem} is the thickness of an elementary ply. For simplicity, the local delamination ratios of both damaged plies verify:

$$\tau\big|_{S_i} = \tau_1^-\big|_{S_i} = \tau_2^-\big|_{S_i} = \tau_1^+\big|_{S_i} = \tau_2^+\big|_{S_i}$$

$$\tau\big|_{S_{i+1}} = \tau_1^-\big|_{S_{i+1}} = \tau_2^-\big|_{S_{i+1}} = \tau_1^+\big|_{S_{i+1}} = \tau_2^+\big|_{S_{i+1}}$$

Table 1. States of microdegradation associated with Fig. 7

ply	microcracking rate ρ	local delamination τ	orientation	thickness
S"+	homogenized	homogenized	θ"+	H"+
S_{i+1}	0.5	0.25	22.5	H_{elem}
S_i	0.35	0.15	-22.5	H_{elem}
S"-	homogenized	homogenized	θ"-	H"-

Taking several configurations of the external plies S"+ and S"- in orientations (θ"+, θ"-) and thicknesses (H"+,H"-), one can note that the intrinsic properties of the micro-meso operators are verified with very good accuracy (< 5%). Fig. 7 illustrates the proof for D_2.

Remark 2: The damage state of the interface depends on the damage state of the adjacent layers, which is in contradiction with the first hypothesis of our standard mesomodel. The development of an improved mesomodel with better consistency with the micromodels is under way.

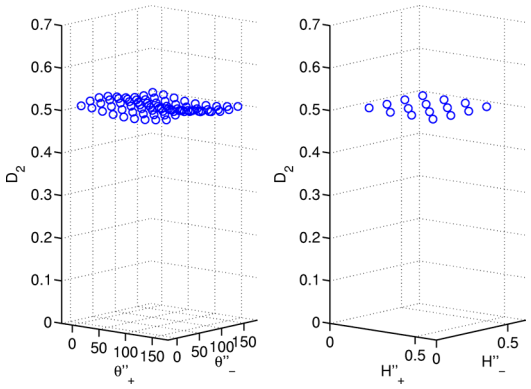

Fig. 7. Intrinsic character of the homogenized damage mesovariable D2

Result 3: There exists a domain of microstates for which the homogenized operator is orthotropic.

The primitive interface mesomodel was assumed to be orthotropic and the bisector directions of the angle θ constituted a natural local reference frame of orthotropic directions. The homogenized operator is also orthotropic if, for a given set of interface parameters, the coupling terms of the potential energy (Result 1) are negligible compared to the diagonal terms.

In order to illustrate this condition, let us consider the basic cell under the four states of degradation defined in Table 2. The degradation of ply S_i is constant whereas the damage state of S_{i+1} varies.

Table 2. The four states of microdegradation associated with Fig. 8

ply	microcracking rate ρ	local delamination τ	orientation	thickness
S''+	homogenized	homogenized	-30	H_{elem}
S_{i+1}	0.4	0.15	+30	H_{elem}
S_i	0.4 or 0.5	0.15 or 0.3	-30	H_{elem}
S''-	homogenized	homogenized	+30	H_{elem}

First, one considers the basic interface problem under a residual stress composed of the three elementary loads $-\tilde{\sigma}.\underline{n}=(\bar{\sigma}_{13}+\bar{\sigma}_{23}+\bar{\sigma}_{33})\underline{n}$ applied simultaneously. The strain energy stored in the interface under this solicitation is taken as the energy reference. Then, one solves six complementary problems for the same cell by considering each elementary loading and the corresponding coupling effects separately. Finally, the energy ratio of each complementary problem is defined as the ratio of the corresponding strain energy of the interface to the energy reference. The results are given in Fig. 8, which shows the distribution of the strain energy among diagonal and coupling terms.

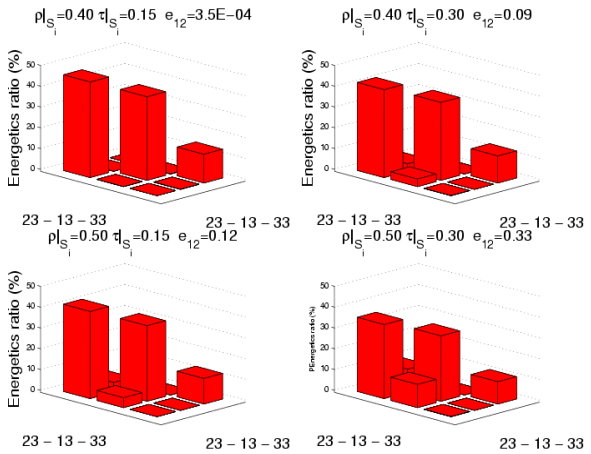

Fig. 8. Distribution of energy among the diagonal and coupling terms

In the particular case of identical microdegradation states in plies S_i and S_{i+1}, the orthotropic character is verified. This condition corresponds to the meso hypothesis that the bisector planes are planes of symmetry of the interface. However, as soon as the states of microdegradation in the plies differ, the symmetries of the interface are broken and coupling between Residuals 23 and 13 appears in the behavior of the damaged interface. This coupling never becomes a prominent factor in our domain of investigation and it will be neglected in further developments. But, if required, one can build a non-orthotropic interface model identified by the results of Fig. 8.

Thus, in the following discussion, the homogenized operator will be expressed as a function of the delamination ratio λ (equal to the ratio of the delaminated area to the total area of the interface) and the average microcracking rate of the adjacent plies ρ:

$$A^{micro}_{interface}(\rho, \lambda)$$

3.3 Micro-meso relations

At this stage, we have proven the relations between the two scales, except near final fracture. It is possible to identify the homogenized operator with the meso-operator. This identification is performed through a virtual testing procedure involving finite element calculations on the microcell. All potential microstates of interface damage are taken into account in the range of value of practical interest specified in Section 2.4.

Result 4: Under pure normal stress loading, the interface's damage does not depend on the transverse microcracks in the plies. D_3 mesodamage is independent of $\rho|_{Si}$ and $\rho|_{Si+1}$.

One can identify the mesodamage D_3 of the interface for any given set of interface parameters. Fig. 9 shows the homogenized D_3 for a given interface ($\theta=60, H_i/H_j=H_{i+1}/H_j=10$) as a function of the delamination ratio λ for three values of the microcracking rate in the adjacent plies.

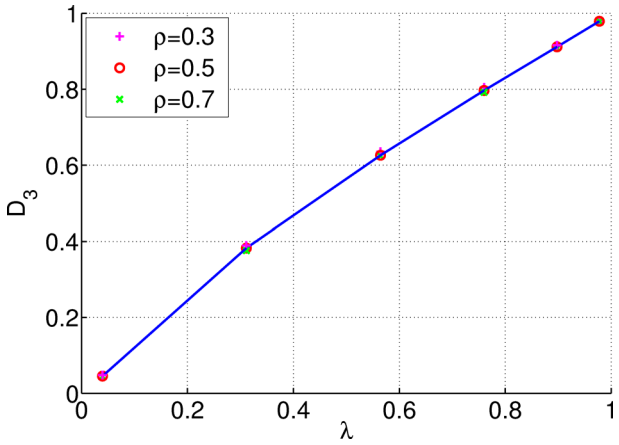

Fig. 9. The interface mesodamage D3 as a function of the delamination ratio

The homogenized mesodamage D_3 is a function of the delamination ratio alone and the microcracking mechanism has no influence on its identification. Similar results would be obtained for any other set of interface parameters. This direct link between the microvariable λ and the interface mesodamage D_3 enables one to choose either D_3 or λ as the delamination variable. Hereafter, the dependence of the other mesodamage variables on local delamination will be expressed in terms of D_3.

Result 5: The mesodamage variables 23 and 13 depend on the transverse cracking scenario of the adjacent plies and on the local delamination scenario. The interaction between the two scenarios is quantified directly.

For any given set of interface parameters, one can identify the mesodamage variables D_1 and D_2 of the interface. Fig. 10 shows the homogenized mesodamage D_2 of a given set of interface parameters (θ=60,$H_i/H_j=H_{i+1}/H_j$=10) as a function of mesodamage D_3 (meso-translation of the local delamination level) for three levels of transverse cracking. The behavior of D_1 is similar. The interactions between the intra- and interlaminar mechanisms have a strong impact on D_1 and D_2 and are quantified directly by the micro-meso link of Fig. 10.

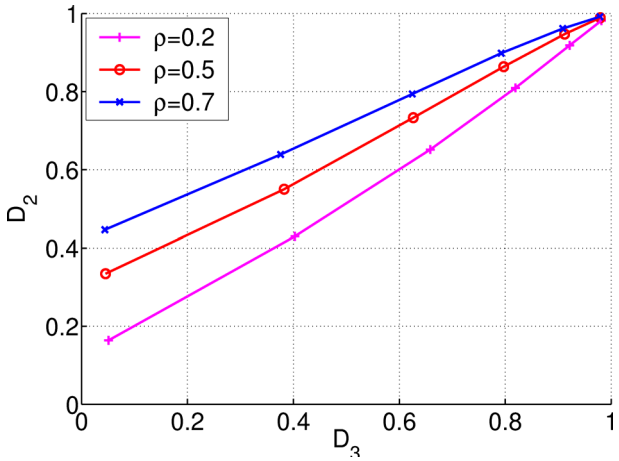

Fig. 10. Interface mesodamage D2 as a function of D3 and the microcracking rate of adjacent plies

4. CONCLUSIONS

We presented a virtual testing procedure for the derivation of relationships between micro- and mesomechanics for the interface modeling of laminates. This bridge between the two scales exists for any stacking sequence, under any loading conditions and for any level of the micromechanisms of damage. We proved that mesodamage D_3 does not depend on the transverse cracking scenario of the adjacent plies. Conversely, mesodamage variables D_1 and D_2 depend on both transverse cracking and local delamination. The resulting interaction effects are quantified on mesodamage variables D_1 and D_2. Thus, , contrary to standard DML, this micro-meso bridge enables one to take the interactions between ply damage and interface damage into account. These results are currently being implemented into an improved mesomodel which will be more consistent with the micromodels. In order to keep things relatively simple, pragmatic rules will be presented in a companion paper.

References:

1. **Flaggs, D.** and **Kural, M.**, "Experimental determination of the in situ transverse lamina strength in graphite/epoxy laminates", *J. Compos. Mater.*, **16** (1982), 103-115.
2. **Hashin, Z.**, "Analysis of cracked laminates: a variational approach", *Mechanical of Materials,* **4** (1985), 121-136.
3. **Boniface, L., Smith, P., Ogin, S.** and **Bader, M.**, "Observations on tranverse ply crack growth in a [0/902]s CFRP laminate under monotonic and cyclic loading", *Proceedings of the 6th International Conference on Composite Materials*, **3** (1987), 156-165.
4. **Laws, N., and Dvorak, G.J**, "Progressive transverse cracking in composite laminates", *J. Compos. Mater.*, 22 (1988), 900-916.
5. **Nairn, J.** and **Hu, S.**, "Matrix microcracking", in: Taljera (Ed.) *Damage Mechanics of Composite Materials* (1994), 187-243.
6. **Joff, R.** and **Varna, J.**, "Analytical modeling of stiffness reduction in symmetric and balanced laminates due to cracks in 90 layer", *Compos. Sci. Technol.*, **59** (1999), 1641-1652.
7. **Crossman, F.** and **Wang, A.**, "The dependence of transverse cracking and delamination on ply thickness in graphite/epoxy laminates", in: Reifsnider (Ed.) *Damage in composite materials*, ASTM-STP 775, (1982),

118-139.

8. **Nairn, J.** and **Hu, S.**, "The initiation and growth of delamination induces by matrix microcracks in laminated composites", *Int. J. Fracture.* , **57** (1992), 1-24.
9. **Berthelot, J.** and **Le Corre, J.F.**, "A model for transverse cracking and delamination in cross-ply laminates", *Compos. Sci. Technol.*, **60** (2000), 1055-1066.
10. **Nairn, J.** and **Hu, S.**, "The initiation and growth of delamination induces by matrix microcracks in laminated composites", *Int. J. Fracture.* , **57** (1992), 1-24.
11. **Talreja, R.**, "Stiffness Based Fatigue Damage Characterization of Fibrous Composites", in: A.R. Bunsell, et.al, (Eds.) *Advances in Composite Materials*, Oxford: Pergamon Press, **2** (1980), 1732-1739.
12. **Renard, J.** and **Jeggy, T.**, "Modélisation de la fissuration transverse dans les matériaux composites carbone/résine", in : *Groupe de reflexion sur l'endommagement*, Cetim, Senlis (1989), in french.
13. **Ladevèze, P.**, "About the damage mechanic of composites", in: C.Bathias, D.Menk es (Eds.), *Comptes-rendus des JNC5*, Pluralis Publication, Paris, (1986), 667-683, in french.
14. **Ladevèze, P.**, "About a damage mechanics approach", in: D. Baptiste (Ed.), *Mechanics and Mechanisms of Damage in Composite and Multimaterials*, MEP, (1989), 119-142.
15. **Herakovich, C.**, *Mechanics of Fibrous Composites*, J. Wiley, (1998).
16. **Ladevèze, P.** and **Lubineau, G.**, "On a damage mesomodel for laminates: micro-meso relationships, possibilities and limits", *Compos. Sci. Technol.*, **61**/15 (2001), 2149-2158.
17. **Ladevèze, P.** and **Lubineau, G.**, "On a damage mesomodel for laminates: micromechanics basis and improvement", *Mech. Mater.*, **35** (2002) 763-775.
18. **Ladevèze, P.** and **Lubineau, G.**, "An enhanced mesomodel for laminates based on micromechanics", *Compos. Sci. Technol.*, **62** (2002), 533-541.
19. **Lagattu, F.** and **Lafarie-Frénot, M.**, "Variation of PEEK matrix crystallinity in APC- 2 composite subjected to large shearing deformation", *Compos. Sci. Technol.*, **60** (2000), 605-612.
20. **Ladevèze, P.** and **Le Dantec, E.**, "Damage modeling of the elementary ply for laminated composites", *Compos. Sci. Technol.*, **43** (1992), 257-267.
21. **Allix, O. and Ladevèze, P.,** "Interlaminar interface modelling for the prediction of laminate delamination"**,** *Composite Structures***, 22** (1992), 235-242.
22. **Allix, O., Bahlouli, N., Cluzel** and **C., Perret,** "Modelling and identification of temperature-dependent mechanical behaviour of the elementary ply in carbon/epoxy laminates", *Compos. Sci. Technol.*, **56** (1996), 883-888.
23. **Allix, O., Lévèque, D., Perret, L.,** "Interlaminar interface model identification and forecast of delamination in composite laminates", *Compos. Sci. Technol.*, **56** (1998), 671-678.
24. **Allix, O.,** "Interface damage mechanics: application to delamination", *Continuum Damage Mechanics of Materials and Structures*, O. Allix and F. Hild, Elsevier, (2002), 295-324.
25. **Ladevèze, P.**, **Lubineau, G.** and **Marsal, D.**, "Towards a bridge between the micro- and the mesomechanics of delamination for laminated composites", *Compos. Sci. Technol.*, to appear 2004.